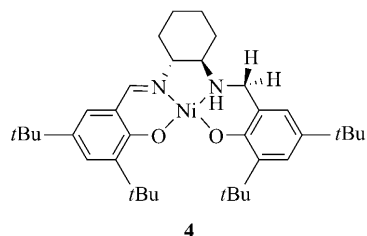
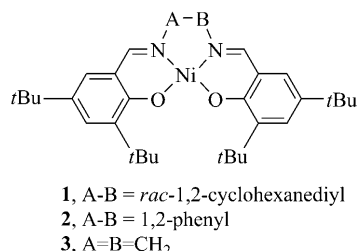


Ligand Radical Localization in a Nonsymmetric One-Electron Oxidized Ni^{II} Bis-phenoxide Complex

Tim Storr,^[a, b] Pratik Verma,^[a] Yuichi Shimazaki,^{*[c]} Erik C. Wasinger,^[d] and T. Daniel P. Stack^{*[a]}

The interplay of electronic structure and reactivity in transition-metal complexes is an area of considerable research effort.^[1,2] The cooperative effect of redox-active ligands and metal sites in enzymatic systems,^[3] and more recently in synthetic systems,^[4] adds significant flexibility to catalyst function. Depending on the relative energies of the redox-active orbitals, metal complexes with proradical ligands can exist in a limiting description as a metal–ligand radical ($M^{n+}(L^\cdot)$) or a high-valent metal complex ($M^{(n+1)+}(L^-)$). In certain cases, subtle changes to the system through variation of the ligand field, or temperature is sufficient to shift the oxidation locus.^[5,6] Recent work in this area has focused on bis-(salicylidene)diamine complexes **1–3** (Scheme 1).^[6–11] The one-electron oxidized Ni derivatives exist in the ligand radical form $Ni^{II}(L^\cdot)$ in solution and the solid state, however the addition of exogenous ligands to $Ni^{II}(L^\cdot)$ in solution results in a shift in the oxidation locus to the $Ni^{III}(L^{2-})$ form.^[7–10] The oxidized Cu derivative of **1** exists as the high-valent metal complex in the solid state. In solution this complex exhibits temperature-dependent valence tautomerism between the ligand radical and high-valent metal forms,



Scheme 1. Nickel bis-phenoxide complexes.

demonstrating the nearly isoenergetic nature of these two species.^[6]

Oxidation studies to date have centered on symmetric bis(salicylidene)diamine complexes, resulting in full delocalization of the radical over the ligand framework. Interestingly, recent work has shown that the oxidized Pd analogue of **1** exhibits partial radical localization on one of the two phenolates as this metal ion limits coupling between the redox-active ligands.^[12] Intrigued by this example, we have synthesized the Ni analogue of a Salalen ligand **4**,^[13] a nonsymmetric variant of **1**.^[14] We hypothesized that the reduced amino-phenolate of **4** would undergo a one-electron oxidation at a lower potential than the iminophenolate, resulting in a localized ligand radical complex. Preferential redox tuning of phenolate ligands has been demonstrated previously in a functional model of galactose oxidase.^[15]

Compound **4** exhibits two reversible redox couples by cyclic voltammetry ($E_{1/2}^1 = 0.13$ V and $E_{1/2}^2 = 0.56$ V vs. Fc⁺/Fc; Fc: ferrocene; see Figure S1 in the Supporting Informa-

[a] Prof. T. Storr, P. Verma, Prof. T. D. P. Stack

Department of Chemistry, Stanford University
 Stanford, CA 94305 (USA)
 Fax: (+1) 650-725-0259
 E-mail: stack@stanford.edu

[b] Prof. T. Storr

Present address: Department of Chemistry
 Simon Fraser University
 Burnaby, BC, V5A-1S6 (Canada)

[c] Prof. Y. Shimazaki

College of Science, Ibaraki University
 Bunkyo, Mito, 310-8512 (Japan)
 Fax: (+81) 29-228-8403
 E-mail: yshima@mx.ibaraki.ac.jp

[d] Prof. E. C. Wasinger

California State University–Chico
 Chico, CA 95929 (USA)

Supporting information for this article is available on the WWW under <http://dx.doi.org/10.1002/chem.201001401>.

tion). The first oxidation for **4** occurs at a potential 0.3 V lower than that for **1**, and compares well with the electrochemistry of a Cu tetrahydrosalen complex.^[16] This is attributed to oxidation of the more electron-rich aminophenolate. Treatment of **4** in CH_2Cl_2 with one equivalent of the oxidants AgSbF_6 ($E_{1/2}=+0.65$ V vs. Fc^+/Fc), thianthrenyl radical [thianthrene] $^{+•}$ SbF_6^- ($E_{1/2}=+0.89$ V vs. Fc^+/Fc), or $(\text{NH}_4)_2\text{Ce}(\text{NO}_3)_6$ results in an immediate color change from red-brown to green, signifying formation of **4⁺**. AgSbF_6 as the chemical oxidant provides crystals of **4⁺** SbF_6^- suitable for X-ray analysis (Figure 1).^[13]

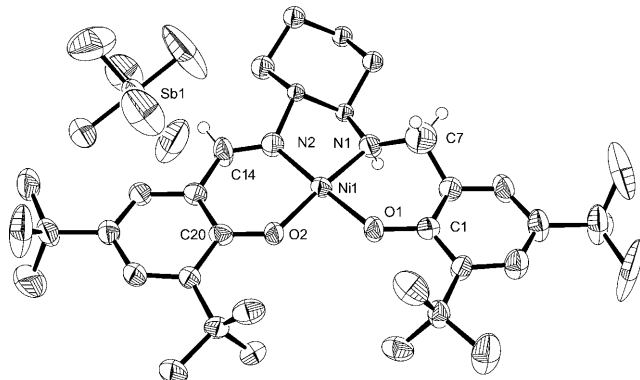


Figure 1. Molecular structure of **4⁺** SbF_6^- (50% probability ellipsoids). Selected interatomic distances [\AA] and angles [$^\circ$]: Ni1–N1 1.872(5), Ni1–N2 1.824(5), Ni1–O1 1.883(4), Ni1–O2 1.823(3), C1–O1 1.365(6), C20–O2 1.329(6), N1–C7 1.472(2), N2–C14 1.283(7); N1–Ni1–N2 86.7(2), O1–Ni1–O2 84.2(1), N1–Ni1–O1 93.3(2), N2–Ni1–O2 95.3(2).

The structures of **4** (see Figure S2 in the Supporting Information) and **4⁺** possess a slightly distorted square-planar geometry about the Ni center, similar to **1** and **1⁺**. While the coordination sphere of **1** contracts symmetrically upon oxidation to **1⁺**,^[10] the Ni coordination sphere of **4⁺** is nonsymmetric (Table 1), with considerable lengthening of the am-

Table 1. Experimental and calculated (in parentheses) coordination sphere metrical parameters for the complexes in \AA .

Ni–O1	Ni–O2	Ni–N1	Ni–N2
4 1.846 (1.876)	1.841 (1.861)	1.845 (1.945)	1.845 (1.877)
4⁺ 1.883 (1.892)	1.823 (1.836)	1.872 (1.951)	1.824 (1.854)

nophenolate Ni–O1 bond by 0.04 \AA in comparison to **4**. The lengthening of the Ni–O1 bond is consistent with a decrease in electron-donating ability of a phenoxy ligand relative to that of phenolate,^[17,18] indicating localized oxidation of the aminophenolate. A similar nonsymmetric coordination environment was observed in the X-ray structure of the Pd analogue of **1⁺**.^[12] DFT calculations^[19] of **4** and **4⁺** reproduce the observed coordination sphere asymmetry in the oxidized form (Table 1). Interestingly, an elongation of the C–O bond lengths is observed upon oxidation of **4** to **4⁺**, instead

of the contraction expected for a phenoxy radical with semi-quinone character.^[17,20]

The EPR spectrum of **4⁺** in CH_2Cl_2 at 77 K exhibits a broad ($S=1/2$) signal with a $g_{\text{iso}}=2.018$ (Figure 2a), indicating that the unpaired electron is ligand-based. The measured

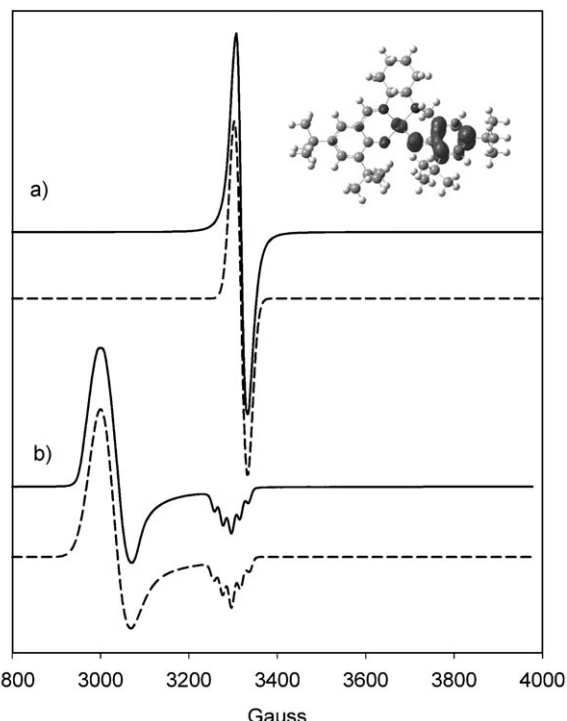


Figure 2. X-band EPR spectra of **4⁺** recorded in frozen CH_2Cl_2 at 77 K (experimental spectra: solid lines; simulations: dashed lines): a) 1 mm **4⁺**, b) 1 mm **4⁺** + 20 equiv pyridine. Inset: Calculated spin density plot for **4⁺**, showing localization of the unpaired electron on the more electron-rich aminophenolate.

g value is lower than that for **1⁺** ($g_{\text{iso}}=2.045$)^[10] indicating a smaller contribution of metal d orbitals (mostly d_{yz}) to the SOMO of **4⁺**, and greater ligand-radical character. This result corresponds well with the lower calculated Ni spin density (Figure 2 inset) for **4⁺** (5%), in comparison to that for **1⁺** (10%).^[21] These results suggest that the electronic coupling between the two redox-active phenolates, mediated, presumably through a hole transfer superexchange mechanism involving the Ni d_{yz} orbital,^[2,10,12] is reduced substantially in **4⁺** as compared to that in **1⁺** (vide infra).

Addition of 20 equivalents of pyridine to **4⁺** at 233 K and subsequent cooling to 77 K results in an anisotropic EPR pattern (Figure 2b) that is consistent with formation of a Ni^{III} species $[\mathbf{4}(\text{py})_2]^{+}$ ($g_x=g_y=2.230$, $g_z=2.032$, $A_z=19 \times 10^{-4} \text{ cm}^{-1}$, $g_{\text{av}}=2.16$). This result is consistent with modulation of the ligand field upon axial binding of pyridine, and a consequent shift in the locus of oxidation to form a Ni^{III} complex.^[8–10]

Ni K-edge X-ray absorption spectroscopy (XAS) was used to further probe the metal oxidation state and structure of frozen solutions of **4**, **4⁺**, and $[\mathbf{4}(\text{py})_2]^{+}$ (Figure S3 in the

Supporting Information). The Ni K-edge 1s → 3d transition, or pre-edge, is a successful indicator of Ni oxidation state,^[22] and the similar energies of the pre-edge feature for **4** (8332.0 eV) and **4⁺** (8331.9 eV) are consistent with a Ni^{II} oxidation state for both complexes. The shift of the pre-edge to higher energy for [**4(py)₂**]⁺ (8332.4 eV) signifies oxidation to Ni^{III}, matching the EPR results (vide supra).

The UV-Vis-NIR spectra of **4** is typical of a low-spin d⁸ square-planar metal complex, and changes substantially upon oxidation to **4⁺** (Figure 3). The spectrum of **4⁺** exhib-

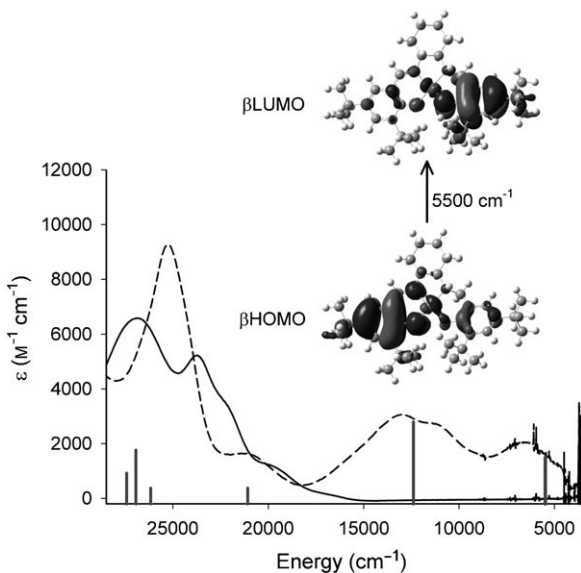


Figure 3. Electronic absorption spectra of 0.08 mm solutions of **4** (solid line) and **4⁺** (dashed line) in CH₂Cl₂ at 298 K. Calculated transitions shown as vertical lines. Inset: TD-DFT assignment (β -HOMO → β -LUMO) of the lowest energy NIR transition (5500 cm⁻¹) for **4⁺**.^[13]

its a new intense band at 25000 cm⁻¹ (9300 M⁻¹ cm⁻¹), and low-energy bands at 13000 cm⁻¹ (3000 M⁻¹ cm⁻¹), 11300 cm⁻¹ (shoulder; 2700 M⁻¹ cm⁻¹), and 6500 cm⁻¹ (2000 M⁻¹ cm⁻¹). The absence of low-energy transitions (<12000 cm⁻¹) in **4** and [**4(py)₂**]⁺ (see Figure S4 in the Supporting Information) indicates that the low-energy bands are associated with the ligand radical. The lowest energy NIR band is predicted by time-dependent density functional theory (TD-DFT) to be a phenolate to phenoxy intervalence charge transfer (IVCT) transition (Figure 3 inset), and is of much weaker intensity in comparison to the NIR band for the Class III^[23] delocalized mixed-valence complex **1⁺** (4700 cm⁻¹, 21500 M⁻¹ cm⁻¹).^[10] This attenuation in NIR band intensity reflects the limited electronic coupling between the two redox-active phenolates in **4⁺**. The intense band at 25000 cm⁻¹ is assigned to a phenoxy radical π → π* transition.^[24] This band is obscured by other intense LMCT transitions in the absorption spectrum of **1⁺**.^[9,11]

The resonance Raman (rR) spectra of **4** and **4⁺** (Figure 4) exhibit key differences upon oxidation, consistent with localization of the ligand radical on the Raman timescale. Vibra-

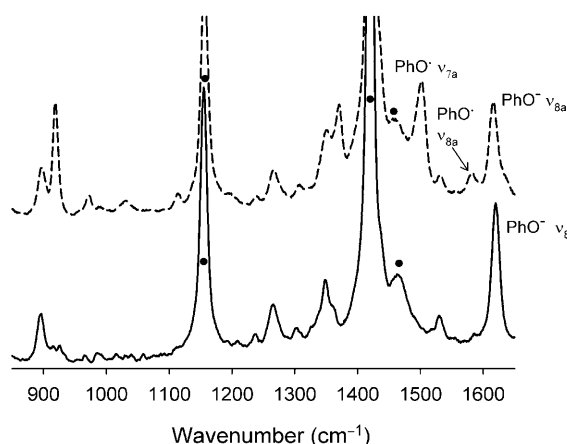


Figure 4. Resonance Raman (rR) spectra of **4** (solid line) and **4⁺** (dashed line) in CH₂Cl₂ at 213 K ($\lambda_{\text{ex}}=413$ nm). Solvent = ●.

tional modes resonant with both phenoxyl π → π* and phenolate-Ni^{II} LMCT transitions are observable in the spectrum of **4⁺**. The features at 1501 and 1581 cm⁻¹ are attributed to characteristic phenoxyl radical C–O stretching, v_{7a} , and C_{ortho}–C_{meta} stretching, v_{8a} , modes respectively.^[25] The rR intensity ratio, $I(v_{8a})/I(v_{7a}) \geq 1$, is often used as a spectral marker for metal-coordinated phenoxyl radicals with p-methoxy substituents.^[24] However, the *tert*-butyl substituents employed in this work may minimize the semi-quinoid character of phenoxyl radicals, and the elongated Ni–O1 bond length could further influence the enhancement of the v_{8a} mode.^[24,26] A combination of these factors presumably leads to the reduced intensity of v_{8a} relative to v_{7a} observed in **4⁺**; a similar intensity pattern is reported for a Ni^{II}–phenoxyl radical complex with the same *tert*-butyl substitution pattern.^[27]

The phenolate/phenoxyl radical v_{8a} mode in **1⁺**^[9] is red-shifted by 22 cm⁻¹ (1625 cm⁻¹ to 1605 cm⁻¹) in comparison to the phenolate v_{8a} mode in **1**,^[28] consistent with delocalization of the ligand radical for **1⁺** on the Raman timescale. The feature at 1615 cm⁻¹ in **4⁺**, assigned to the phenolate v_{8a} mode, is only red-shifted by 4 cm⁻¹ in comparison to the corresponding feature in **4**.^[28] These rR results further support a localized ligand radical description for **4⁺**.

In summary, we have characterized the electronic structure of a nonsymmetric one-electron oxidized Ni^{II} bis-phenoxide complex **4⁺**. While the symmetric derivative **1⁺** is a Class III mixed-valence species, **4⁺** is best described as a Class II mixed valence species due to localization of the ligand radical on the more electron rich amino-phenolate.

Experimental Section

Synthesis of **4⁺SbF₆⁻:** Compound **4** (0.097 g, 0.16 mmol) was dissolved in CH₂Cl₂ (3 mL), and solid AgSbF₆ (0.055 g, 0.16 mmol) was added. A bright green suspension formed immediately. After 1 h the mixture was filtered through celite and the solvent was removed in vacuo to afford a green solid. The material was recrystallized from CH₂Cl₂/pentane to afford **4⁺SbF₆⁻** as green block-like crystals. Magnetic susceptibility;

(Evan's Method) $\mu_{\text{eff}} = 1.6$ BM. Elemental analysis (%) calcd for $\text{C}_{36}\text{H}_{54}\text{N}_2\text{O}_2\text{NiSbF}_6$: C 51.40, H 6.47, N 3.33; found: C 51.56, H 6.18, N 3.28.

X-ray details for **4** and **4⁺** SbF_6^- are available in the Supporting Information. CCDC-770780 and CCDC-770781 contain the supplementary crystallographic data for this paper. These data can be obtained free of charge from The Cambridge Crystallographic Data Centre via www.ccdc.cam.ac.uk/data_request/cif Synthetic procedures, X-ray data, computations, electrochemistry, UV/Vis data, X-ray absorption spectroscopy, and Raman analysis are available as Supporting Information.

Acknowledgements

This work was supported by NIH grant GM-50730 (T.D.P.S.), the CSUC College of Natural Science (E.C.W.), an NSERC post-doctoral scholarship (T.S.), and a Grant-in-Aid for Scientific Research No. 17750055 (Y.S.). Dr. Allen Oliver is thanked for X-ray analysis. SSRL operations are funded by the DOE, Office of Basic Energy Services. Prof. Fumito Tani, Kusuh University is acknowledged for Raman analysis. Mithi Adhikari is thanked for the solution magnetic measurement of **4⁺**.

Keywords: intervalence complexes • localization • N,O ligands • nickel • oxidation locus

- [1] a) P. Chaudhuri, K. Wieghardt, *Prog. Inorg. Chem.* **2001**, *50*, 151; b) F. Thomas, *Eur. J. Inorg. Chem.* **2007**, 2379; c) C. G. Pierpont, *Coord. Chem. Rev.* **2001**, *216*, 99.
- [2] K. Ray, T. Petrenko, K. Wieghardt, F. Neese, *Dalton Trans.* **2007**, 1552.
- [3] J. Stubbe, W. A. van der Donk, *Chem. Rev.* **1998**, *98*, 705; a) J. W. Whittaker, *Chem. Rev.* **2003**, *103*, 2347.
- [4] a) M. W. Bouwkamp, A. C. Bowman, E. Lobkovsky, P. J. Chirik, *J. Am. Chem. Soc.* **2006**, *128*, 13340; b) P. J. Chirik, K. Wieghardt, *Science* **2010**, *327*, 794; c) M. Königsmann, N. Donati, D. Stein, H. Schonberg, J. Harmer, A. Sreekanth, H. Grutzmacher, *Angew. Chem.* **2007**, *119*, 3637; *Angew. Chem. Int. Ed.* **2007**, *46*, 3567; d) A. I. Nguyen, K. J. Blackmore, S. M. Carter, R. A. Zarkesh, A. F. Heyduk, *J. Am. Chem. Soc.* **2009**, *131*, 3307; e) M. R. Ringenberg, S. L. Kokatam, Z. M. Heiden, T. B. Rauchfuss, *J. Am. Chem. Soc.* **2008**, *130*, 788; f) W. I. Dzik, J. N. H. Reek, B. de Bruin, *Chem. Eur. J.* **2008**, *14*, 7594; g) D. G. H. Hetterscheid, J. Kaiser, E. Reijerse, T. P. J. Peters, S. Thewissen, A. N. J. Blok, J. M. M. Smits, R. de Gelder, B. de Bruin, *J. Am. Chem. Soc.* **2005**, *127*, 1895.
- [5] a) D. Dolphin, T. Niem, R. H. Felton, I. Fujita, *J. Am. Chem. Soc.* **1975**, *97*, 5288; b) H. Ohtsu, K. Tanaka, *Angew. Chem.* **2004**, *116*, 6461; *Angew. Chem. Int. Ed.* **2004**, *43*, 6301; c) F. F. Puschmann, J. Harmer, D. Stein, H. Ruegger, B. de Bruin, H. Grutzmacher, *Angew. Chem.* **2010**, *122*, 395; *Angew. Chem. Int. Ed.* **2010**, *49*, 385.
- [6] T. Storr, P. Verma, R. C. Pratt, E. C. Wasinger, Y. Shimazaki, T. D. P. Stack, *J. Am. Chem. Soc.* **2008**, *130*, 15448.
- [7] O. Rotthaus, O. Jarjayes, F. Thomas, C. Philouze, C. P. Del Valle, E. Saint-Aman, J. L. Pierre, *Chem. Eur. J.* **2006**, *12*, 2293.
- [8] O. Rotthaus, F. Thomas, O. Jarjayes, C. Philouze, E. Saint-Aman, J. L. Pierre, *Chem. Eur. J.* **2006**, *12*, 6953.
- [9] Y. Shimazaki, F. Tani, K. Fukui, Y. Naruta, O. Yamauchi, *J. Am. Chem. Soc.* **2003**, *125*, 10512.
- [10] T. Storr, E. C. Wasinger, R. C. Pratt, T. D. P. Stack, *Angew. Chem.* **2007**, *119*, 5290; *Angew. Chem. Int. Ed.* **2007**, *46*, 5198.
- [11] O. Rotthaus, O. Jarjayes, C. P. Del Valle, C. Philouze, F. Thomas, *Chem. Commun.* **2007**, 4462.
- [12] Y. Shimazaki, T. D. P. Stack, T. Storr, *Inorg. Chem.* **2009**, *48*, 8383.
- [13] See the Supporting Information for details.
- [14] a) K. Nakano, M. Nakamura, K. Nozaki, *Macromolecules* **2009**, *42*, 6972; b) A. Berkessel, M. Brandenburg, E. Leitterstorff, J. Frey, J. Lex, M. Schafer, *Adv. Synth. Catal.* **2007**, *349*, 2385.
- [15] F. Thomas, G. Gellon, I. Gautier-Luneau, E. Saint-Aman, J. L. Pierre, *Angew. Chem.* **2002**, *114*, 3173; *Angew. Chem. Int. Ed.* **2002**, *41*, 3047.
- [16] R. C. Pratt, T. D. P. Stack, *J. Am. Chem. Soc.* **2003**, *125*, 8716.
- [17] a) L. Benisvy, A. J. Blake, D. Collison, E. S. Davies, C. D. Garner, E. J. L. McInnes, J. McMaster, G. Whittaker, C. Wilson, *Chem. Commun.* **2001**, 1824; b) A. Sokolowski, E. Bothe, E. Bill, T. Weyhermüller, K. Wieghardt, *Chem. Commun.* **1996**, 1671.
- [18] L. Benisvy, A. J. Blake, D. Collison, E. S. Davies, C. D. Garner, E. J. L. McInnes, J. McMaster, G. Whittaker, C. Wilson, *Dalton Trans.* **2003**, 1975.
- [19] Gaussian 03, Revision C.02, M. J. Frisch, G. W. Trucks, H. B. Schlegel, G. E. Scuseria, M. A. Robb, J. R. Cheeseman, J. A. Montgomery, Jr., T. Vreven, K. N. Kudin, J. C. Burant, J. M. Millam, S. S. Iyengar, J. Tomasi, V. Barone, B. Mennucci, M. Cossi, G. Scalmani, N. Rega, G. A. Petersson, H. Nakatsuji, M. Hada, M. Ehara, K. Toyota, R. Fukuda, J. Hasegawa, M. Ishida, T. Nakajima, Y. Honda, O. Kitao, H. Nakai, M. Klene, X. Li, J. E. Knox, H. P. Hratchian, J. B. Cross, V. Bakken, C. Adamo, J. Jaramillo, R. Gomperts, R. E. Stratmann, O. Yazyev, A. J. Austin, R. Cammi, C. Pomelli, J. W. Ochterski, P. Y. Ayala, K. Morokuma, G. A. Voth, P. Salvador, J. J. Dannenberg, V. G. Zakrzewski, S. Dapprich, A. D. Daniels, M. C. Strain, O. Farkas, D. K. Malick, A. D. Rabuck, K. Raghavachari, J. B. Foresman, J. V. Ortiz, Q. Cui, A. G. Baboul, S. Clifford, J. Cioslowski, B. B. Stefanov, G. Liu, A. Liashenko, P. Piskorz, I. Komaromi, R. L. Martin, D. J. Fox, T. Keith, M. A. Al-Laham, C. Y. Peng, A. Nanayakkara, M. Challacombe, P. M. W. Gill, B. Johnson, W. Chen, M. W. Wong, C. Gonzalez, J. A. Pople, Gaussian, Inc., Wallingford CT, **2004**.
- [20] V. W. Manner, T. F. Markle, J. H. Freudenthal, J. P. Roth, J. M. Mayer, *Chem. Commun.* **2008**, 256.
- [21] The slight difference in Ni spin density for **1⁺** (10%) in comparison to our previous report (14%; see reference [10]) is due to the use of the 6-311g* basis set (Ni, O, N) in this investigation in comparison to the use of the TZVP basis set of R. Ahlrichs (A. Schafer, H. Horn, R. Ahlrichs, *J. Chem. Phys.* **1992**, *97*, 2571) in the previous report.
- [22] K. Fujita, R. Schenker, W. W. Gu, T. C. Brunold, S. P. Cramer, C. G. Riordan, *Inorg. Chem.* **2004**, *43*, 3324.
- [23] a) M. B. Robin, P. Day, *Adv. Inorg. Chem. Radiochem.* **1967**, *9*, 247; b) D. M. D'Alessandro, F. R. Keene, *Chem. Soc. Rev.* **2006**, *35*, 424.
- [24] R. Schneppf, A. Sokolowski, J. Müller, V. Bachler, K. Wieghardt, P. Hildebrandt, *J. Am. Chem. Soc.* **1998**, *120*, 2352.
- [25] a) J. Radziszewski, M. Gil, A. Gorski, J. Spanget-Larsen, J. Waluk, B. Mroz, *J. Chem. Phys.* **2002**, *116*, 5912; b) J. Spanget-Larsen, M. Gil, A. Gorski, D. M. Blake, J. Waluk, J. G. Radziszewski, *J. Am. Chem. Soc.* **2001**, *123*, 11253.
- [26] G. N. R. Tripathi, R. H. Schuler, *J. Phys. Chem.* **1988**, *92*, 5129.
- [27] Y. Shimazaki, S. Huth, S. Karasawa, S. Hirota, Y. Naruta, O. Yamauchi, *Inorg. Chem.* **2004**, *43*, 7816.
- [28] Selected Raman peaks [cm^{-1}] ($\lambda_{\text{ex}} = 413 \text{ nm}$) **4**: $\tilde{\nu} = 1350$, 1530, 1619 cm^{-1} (ν_{8a}); **4⁺**: 918, 1350, 1370, 1501 ($\text{PhO}' \nu_{7a}$), 1530, 1581 ($\text{PhO}' \nu_{8a}$), 1615 cm^{-1} (ν_{8a}); **1**: 1351, 1533, 1627 cm^{-1} (ν_{8a}); **1⁺**: 1370, 1504 ($\text{PhO}' \nu_{7a}$), 1605 cm^{-1} ($\text{PhO}' \nu_{8a}$).

Received: April 7, 2010

Published online: July 19, 2010